Non-Symmetry-Breaking Ground State of the $S = 1$ Heisenberg Model on the Kagome lattice

Satoshi Nishimoto[1] and Masaaki Nakamura[2]

[1]*Institute for Theoretical Solid State Physics, IFW Dresden, Helmholtzstrasse 20, 01069 Dresden, Germany*
[2]*Institute of Industrial Science, the University of Tokyo, Meguro-ku, Tokyo, 153-8505, Japan*

(Dated: September 24, 2014)

The $S = 1$ antiferromagnetic Heisenberg model on a Kagome lattice is studied using the density-matrix renormalization group method. To identify the ground state, we take four kinds of clusters into account; periodic, cylindrical, and two open ones. The hexagonal singlet solid (HSS) and triangular valence bond solid (TVBS) states are artificially generated by modulating edge shapes of the open clusters. We find that the energy par sites of the HSS state is $e_0 = E_0/N = -1.41095$, which is readily lower than that of the TVBS state ($e_0 = -1.3912 \pm 0.0025$). This agrees well with those of the cylindrical ($e_0 = -1.40988$) and periodic ($e_0 = -1.409 \pm 0.005$) clusters, where no assumption as to the ordering is posed. Thus, we conclude that the HSS picture is consistent to describe the ground state of the $S = 1$ Kagome Heisenberg model. This is further confirmed by finding non-symmetry-breaking state in the calculations of the dimer-dimer correlation functions as well as the entanglement entropy of cylindrical clusters. Finally, we estimate the single-triplet energy gap: The HSS ground state has $\Delta = 0.1919$, while the TVBS excited state has a larger one $\Delta = 0.2797$.

PACS numbers: 75.10.Jm, 75.10.Kt, 75.40.Mg

arXiv:1409.5870v2 [cond-mat.str-el] 23 Sep 2014

For a long time, frustrated spin systems have been fascinating subjects of research for discovering new physics [1]. Among them a system attracting the most attention in recent years is Kagome antiferromagnetic Heisenberg (KAH) model, and a lot of experimental and theoretical studies on the Kagome system have been carried out, assisted by the improvement of research techniques.

In the $S = 1/2$ KAH system, one of the most striking finding is the fact that this ground state is characterized as a Z_2 spin liquid [2, 3]. The experimental realization of spin liquid has been also demonstrated in the herbertsmithite $ZnCu_3(OD)_6C_{l2}$ [4]. Theoretically, it is still debated whether the ground state is gapless [5] or gapped with very small energy gap [2, 6–8]. Another notable feature is the appearance of a series of plateaus in the magnetization process [8, 9]. Of particular interest is a possible Z_3 spin liquid plateau at 1/9 magnetization [8]. Thus the $S = 1/2$ KAH model exhibits a variety of phases, although it is a simple Heisenberg system consisting only of the nearest-neighbor exchange couplings.

We here turn our attention on an $S = 1$ version of the KAH model. It would be a natural continuation of the study on the KAH system. The Hamiltonian is written as

$$H = J \sum_{\langle ij \rangle} \mathbf{S}_i \cdot \mathbf{S}_j \qquad (1)$$

where $\mathbf{S}_i$ is a spin-one operator at site i, and the summation is taken for nearest neighbours $\langle ij \rangle$. J is the antiferromagnetic exchange integral and we set $J = 1$ hereafter. From the theoretical point of view, a very interesting point is an extension of valence-bond solid (VBS) picture [10] to two-dimension. Firstly, the triangular VBS (TVBS) state was suggested as a ground state by the perturbation expansion around the complete TVBS limit [11]. After that, according to the analysis based on the exact diagonalization and variational method, it was claimed that hexagonal-singlet solid (HSS) ground state is realized [12] (see Fig. 1). Moreover,

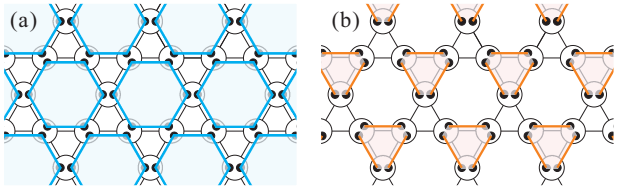

FIG. 1. Schematic illustrations of valence-bond solid (VBS) state in the $S = 1$ Kagome antiferromagnetic Heisenberg model: (a) the hexagonal-singlet solid (HSS) and (b) the triangular VBS states. Blue (red) line indicates a spin-singlet formation in six (two) $S = 1/2$ variables.

a resonating AKLT loop (RAL) state has been recently suggested as an alternative candidate [13]. The ground state of the $S = 1$ KAH model is still an open issue. So far, several materials have been synthesized as possible realizations of the $S = 1$ KAH system, e.g., m-MPYNN·BF_4 [14, 15], $KV_3Ge_2O_9$ [16], $[C_6N_2H_8][NH_4]_2[Ni_3F_6(SO_4)_2]$ [17], and $NaV_3(OH)_6(SO_4)_2$ [18]. Further experimental observations are strongly expected.

In this Letter, the ground state of the $S = 1$ KAH model is determined. We use the density-matrix renormalization group (DMRG) method, which enables us to study large-size clusters. For this aim, we exploit four kinds of clusters shown in Fig. 2. Up to about 10000 density-matrix eigenstates are kept in the renormalization procedure and the discarded weight is below 10^{-4} even for the most difficult case, namely, 36-site cluster under the periodic boundary conditions (PBC). First, by calculating the dimer-dimer correlation functions and entanglement entropy with the cylindrical clusters, we find that the translational symmetry is not broken in the ground state.It is further confirmed with the PBC cluster. Next, we *intentionally* produce the HSS and TVBS states by modulating the edge condition of open clusters (see below for details). It enables

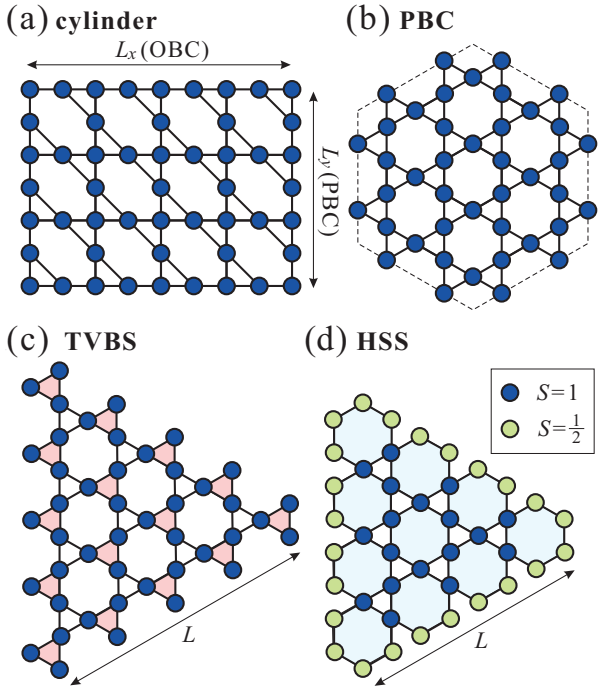

FIG. 2. Lattices used for the DMRG calculations: (a) A cylindrical cluster, denoted as XC6-3, where periodic (open) boundary conditions is applied in the vertical (horizontal) direction. (b) A PBC cluster with $N = 36$ sites. Other PBC clusters are shown in the Supplemental material. (c),(d) Open clusters for obtaining the TVBS and HSS states, respectively.

us to compare their energies directly. The lowest-state energy calculated with the HSS cluster is $E_0/N \equiv e_0 = -1.41095$ and it is in good agreement with those of the cylindrical ($e_0 = -1.40988$) and PBC ($e_0 = -1.409 \pm 0.005$) clusters. It is quite reasonable because the HSS state is a non-symmetry-breaking one. Moreover, it is striking that the energy estimated with the TVBS cluster ($e_0 = -1.3912 \pm 0.0025$) is decidedly higher than the others. Thus, we verify the HSS state to be the ground state of the $S = 1$ KAH model. Finally, we estimate the single-triplet gap. The ground state, i.e., the HSS state, has a gap $\Delta = 0.1919$; while, the TVBS state as an excited eigenstate has a larger gap $\Delta = 0.2797$.

Let us start with the cylindrical cluster [Fig. 2(a)]. We here use a type of cylinder denoted as XC6-3, the notation of which was defined in previous works on the $S = 1/2$ KAH system [2, 6]. The reason for choosing it is related to the shape of both edges. In general, an open edge exerts a critical influence on the formation of plaquette or bond singlets. If the edge consists of either triangles or hexagons, the TVBS or HSS state may be artificially favoured in our system (1). Such a signature was also identified in the $S = 1/2$ KAH model [2, 19]. This problem should be avoided by choosing a XCn-(n/2) or YCn type of cylinder, where both triangles and hexagons are *equally* arranged at the open edges (see Supplement). In other words, the TVBS and HSS states could be intentionally stabilized by modulating the shape of open edges in a (small) cluster. This *technique* is used in the latter part of this Letter. For instance, the same technique was used to detect the plaquette VBS state in the J_1-J_2 honeycomb Heisenberg model [20].

In order to check the configuration of singlet valence bonds, we calculate the dimer-dimer correlation functions defined by

$$C_{(i,j)(k,l)} = 4[\langle(\mathbf{S}_i \cdot \mathbf{S}_j)(\mathbf{S}_k \cdot \mathbf{S}_l)\rangle - \langle \mathbf{S}_i \cdot \mathbf{S}_j \rangle \langle \mathbf{S}_k \cdot \mathbf{S}_l \rangle]. \quad (2)$$

In Fig. 3(a) the values of the dimer-dimer correlation for each bond are shown with fixing one reference dimer bond. Blue and red links denote positive and negative correlations. It seems that the patterns for the sign of correlations does not exhibit any spatial periodicity. In addition, the correlation decays exponentially with distance of two bonds, as plotted in Fig. 3(b). It clearly indicates the absence of symmetry-breaking order associated with dimer formations. A similar feature is also observed in the PBC clusters [Fig. 3(d)] Moreover, to make sure, we examine the von Neumann entanglement entropy (EE) $S_L(l) = -\mathrm{Tr}_l \rho_l \log \rho_l$, where $\rho_l = \mathrm{Tr}_{L-l}\rho$ is the reduced density matrix of the subsystem and ρ is the full density matrix of the whole system [3, 21]. We plot the value of $S_{\frac{L}{2}}$ as a function of the circumference of the cylinder L_y. The values should follow a relation $S(L_y) = \alpha L_y - \gamma$, where α is a constant and $\gamma = \ln D$ is the topological entropy with dimension D [22, 23]. By the fitting of our data with the equation, we obtain $\gamma = 0.0014$ in the $L_y \to 0$ limit. This suggests that the system is in a topologically trivial phase, i.e., a unique ground state, and it is consistent to the results of the dimer-dimer correlation functions.

Next, we consider the TVBS state. As mentioned above, an ordered state like the symmetry-breaking TVBS state can be forcibly stabilized as the lowest state in a small cluster by taking a proper edge condition. However, we have to take notice the following two points to determine if the lowest state is really the ground state when this artificial technique is applied: (i) the ordering survives in the thermodynamic limit, (ii) the energy of the ordered state remains lowest among all eigenstates in the thermodynamic limit. If it is not the case, a level crossing with the true ground state occurs at some larger cluster. One possible realization of the TVBS cluster is shown in Fig. 2(c). For this cluster we present the values of the nearest-neighbour spin-spin correlations $\langle -\mathbf{S}_i \cdot \mathbf{S}_j \rangle$ in Fig. 3(e). A link with larger (smaller) value than that of the next bonds is coloured in red (blue). A TVBS configuration is obviously seen. Furthermore, with increasing the system size, the spin gap is smoothly scaled to a finite value $\Delta = 0.2797$ at $1/L \to 0$ (see the inset of Fig. 3(f)). The spin gap is evaluated as the energy difference between the lowest singlet and the first excited triplet states. Hence, the TVBS state is confirmed to survive in the thermodynamic limit. We also make certain that this state is indeed of the TVBS with triangular three-dimer formations. For this purpose, we modulate the exchange couplings as $(1+\delta)J$ and $(1-\delta)J$ for red and blue bonds in Fig. 3(e), respectively ($0 \le \delta \le 1$). Figure 3(f) shows the spin gap as a function of δ. In the isolated triangle limit ($\delta = 1$), the lowest state is exactly described by

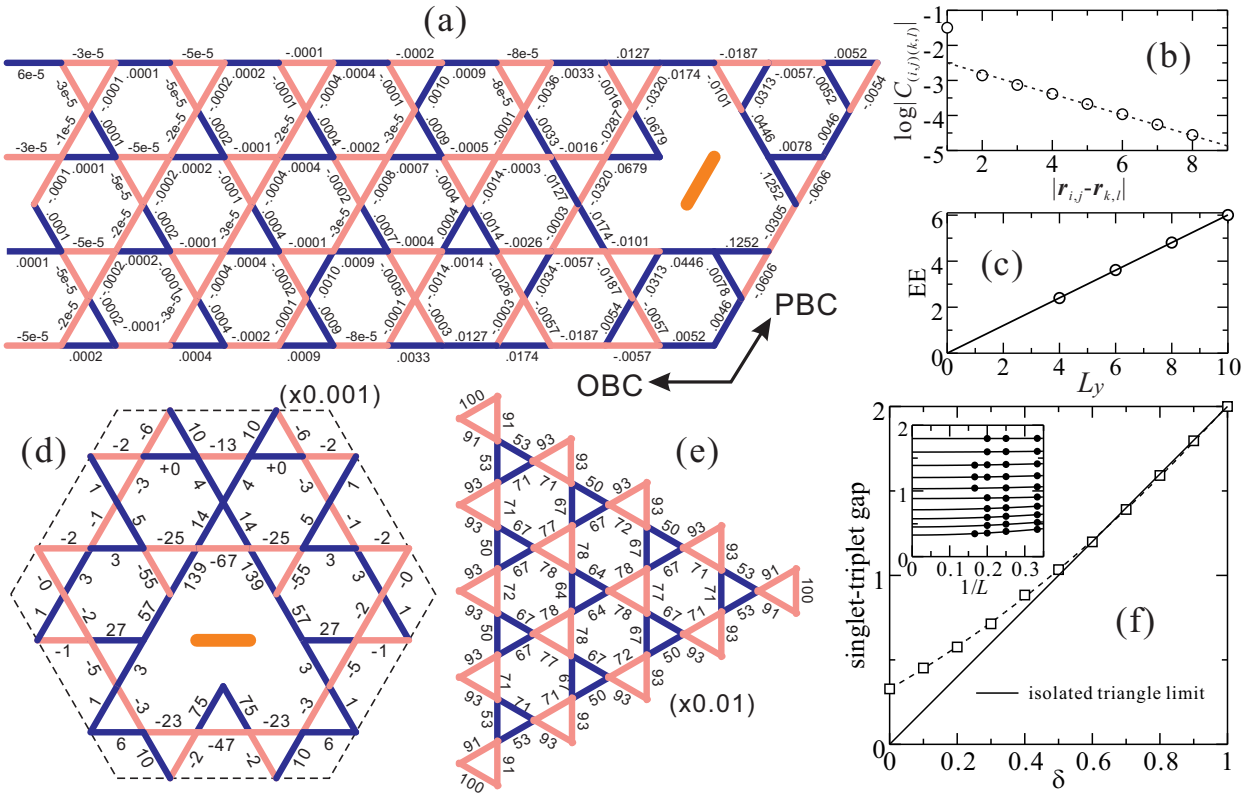

FIG. 3. (a) Dimer-dimer correlation functions for the XC6-3 cylinder with $L_y = 24$. The reference bond is indicated by the thick orange line. (b) Semilog plot of the absolute value of dimer-dimer correlation functions with distance from the reference bond. (c) Entanglement entropy with L_y. The $L_x \to \infty$ limit has been already taken. (d) Dimer-dimer correlation functions for the PBC cluster ($N = 36$). (e) Nearest-neighbour spin-spin correlation functions for the TVBS cluster. (f) Singlet-triplet gap extrapolated to the thermodynamic limit for the modulated TVBS clusters (see text). Inset: the extrapolation scheme as a function of $1/L$.

a direct product of triangular Haldane-gap dimers with three $S = 1$ spins; as δ decreases, the fluctuations between the triangles are increased and the original Hamiltonian is recovered at $\delta = 0$. It is worth noting the spin gap is scaled perfectly by that assuming an isolated triangle, $\Delta = 2\delta$, for a wide range of $\delta(> 0.5)$. This means that the triangular Haldane-gap dimers are quite robust against the inter-triangle fluctuations and the product state may be a good approximation of the TVBS state even at smaller δ. We can further see that no gap closing point exists from $\delta = 1$ to $\delta = 0$, suggesting that the product state is intermittently connected to the TVBS state in the original model (1). Therefore, we can confirm that the TVBS state indeed exists as an eigenstate of the $S = 1$ KAH model.

For identifying the true ground state, it would be a natural step to compare the lowest-state energies calculated with different clusters. In Fig. 4 the finite-size scaling analysis of the energy per site for each cluster is presented. For the TVBS and PBC clusters, the energy is plotted with $1/\sqrt{N}$ as usually assumed for two-dimensional systems. For the cylindrical cluster, we first take the $1/L_x \to 0$ limit followed by the $1/L_y \to 0$ limit. Only the scaling with $1/L_y$ is shown in Fig. 4. We estimate the energy for the TVBS cluster in two different ways; one is simply the total energy divided by the total number of sites ($e_0(N) = E_0(N)/N$) and the other is an average of the neighbouring spin-spin correlations ($e_0(N) = 2\langle \mathbf{S}_i \mathbf{S}_j \rangle$, where the factor 2 comes from the ratio of the number of sites and bonds in the thermodynamic limit). Since one of them is extrapolated from the higher energy side

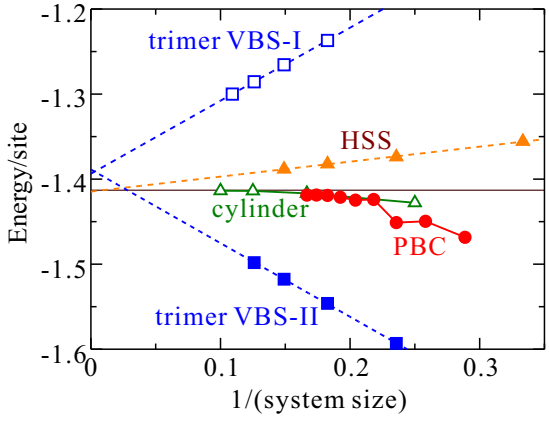

FIG. 4. Extrapolation scheme of the lowest-lying-state energy as a function of $1/L_y$ for the cylindrical cluster and of $1/\sqrt{N}$ for the TVBS, HSS, and PBC clusters. For the cylindrical cluster the $L_x \to \infty$ limits are already taken.

with decreasing $1/L_y$ and the other from the lower side, as seen in Fig. 4, this should make the scaling analysis more reliable. The extrapolated values from the both ways agree very well in the thermodynamic limit and it is estimated as $e_0 = -1.3912 \pm 0.0025$. The energies for the cylindrical and PBC clusters seem to converge rather faster with the system sizes, and they are $e_0 = -1.40988$ and $e_0 = -1.409 \pm 0.005$, respectively, in the thermodynamic limit. Clearly, the energy of the TVBS state is high in number ($\Delta e_0 = 0.02$) compared to those for the other two clusters. We thus argue that the TVBS state exists as an eigenstate but it is not the ground state.

In a similar way as the TVBS state, we can also stabilize the HSS state in a small cluster. One possible realization is shown in Fig. 2(d), where the hexagons are placed at the corners of open cluster. Note that the outer $S = 1$ spins are replaced by $S = 1/2$ spins not to hold extra free spins when all hexagons form singlet plaquettes. By doing this we can easily detect the first excited triplet state by one spin-flip from the lowest state. For the HSS cluster we estimate the energy as an averaged value of the neighbouring spin-spin correlations between the $S = 1$ spins, namely, the outer bonds are excluded. The size-scaling is shown in Fig. 4. The extrapolated value to the thermodynamic limit is $e_0 = -1.41095$. It agrees to those of the cylindrical and PBC clusters within the error bars. Since the HSS state is a non-symmetry-breaking one, it is utterly reasonable.

Although it is not possible to study a RAL state with our method, our estimation of the energy of the HSS state is readily lower than the variational energy of the pure RAL state $e_0 = -1.383$ [13]. Therefore, we conclude that the HSS state is the ground state of the $S = 1$ KAH model. It has been suggested that the TVBS state is the ground state when a certain amount of the second- and third-neighbour antiferromagnetic exchange interactions are taken into account [24]. It is likely to happen because a frustration induced by the second-neighbour interactions naively lifts up the energy of the HSS state.

Finally, we study the spin gap. In Fig. 5 the finite-size-scaling analyses of the spin gap for the used four kinds of clusters are performed. The extrapolated values to the thermodynamic limit are $\Delta = 0.183$, 0.17 ± 0.03, and 0.172 for the cylindrical, PBC, and HSS clusters, respectively. As expected from the above discussion, the three numbers are very close to each other. We thus determine the spin gap of the HSS state, which is the ground state, is $\Delta = 0.178 \pm 0.05$. It is considerably smaller than that of the TVBS state, i.e., $\Delta = 0.2797$. This may imply that the triangular Haldane-gap dimers in the TVBS state is more robust than the hexagonal singlet in the HSS state. Hence, in the TVBS state the spins are strongly screened and the energy gain from the quantum fluctuations between the triangles might be small. Here we shall comment on the spin gap observed in a related material m-MPYNN·BF_4. From the fitting of measured susceptibility with $(\Delta/k_BT)\exp(-\Delta/k_BT)$ at low temperature T, Δ was obtained as ~ 0.2K [14, 15]. This system can be mapped to

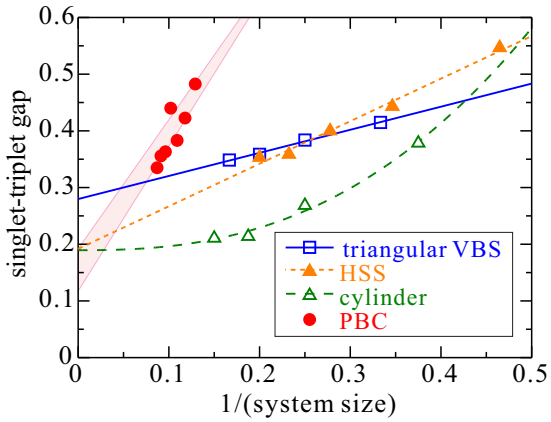

FIG. 5. Extrapolation scheme of the spin gap as a function of $1/L_y$ for the cylindrical cluster, of $1/L$ for the TVBS, HSS, and of $1/\sqrt{N}$ for the PBC clusters. For the cylindrical cluster the limit for $L_x \to \infty$ are already taken.

the $S = 1$ KAH model with $J = 0.65 - 0.95$ K. By our analysis the spin gap is estimated as $\Delta = 0.178J \approx 0.12 - 0.17$K. This value seems to be reasonably close to the experimental one.

In summary, we have studied the $S = 1$ KAH model using the DMRG technique. Four kinds of clusters have been used to determine the ground state. We have succeeded in extracting the ordered HSS and TVBS states by taking unique open clusters. It enabled us to extrapolate their low-lying energies individually to the thermodynamic limit. As a result, we have found that the ground state of the $S = 1$ KAH model is the HSS state and the TVBS state is an excited one. However, their lowest-lying-state energies are very close, and the near degeneracy seems to make it more difficult to detect the true ground state. The dimer-dimer correlation functions and the entanglement entropy for the cylindrical and PBC clusters, where no assumptions for ordering are posed, suggest a non-symmetry-breaking ground state. It also supports the HSS ground state. The singlet-triplet gap of the TVBS state is larger than that of the HSS state. It means that the triangular singlet dimers are more robust than the hexagonal singlet, and the spin are strongly screened. It may prevent lowering of the energy derived by quantum fluctuations between triangular singlet dimers.

We acknowledge Max-Planck-Institut für Festkörperforschung where a part of the numerical calculations has been done.

Note added — In preparing this manuscript we noticed two preprints on the DMRG study of the $S = 1$ KAH model [25, 26]. Although they argued different ground state from our conclusion, the ground-state energy in their calculations agrees with ours very well.

[1] R. Moessner and A. P. Ramirez, Physics Today, pp. 24, February 2006.
[2] S. Yan, D.A. Huse, and S.R. White, Science **332**, 1173 (2011).
[3] H.-C. Jiang, Z. Wang, and L. Balents, Nature Physics **8**, 902 (2012).
[4] T.-H. Han, J. S. Helton, S. Chu, D. G. Nocera, J.A. Rodriguez-Rivera, C. Broholm, and Y. S. Lee, Nature **492**, 406 (2012).
[5] Y. Iqbal, F. Becca, S. Sorella, and D. Poilblanc, Phys. Rev. B **87**, 060405(R) (2013); Y. Iqbal, D. Poilblanc, and F. Becca, Phys. Rev. B **89**, 020407(R) (2014).
[6] S. Depenbrock, I. P. McCulloch, and U. Schollwöck, Phys. Rev. Lett.**109**, 067201 (2012).
[7] H. C. Jiang, Z. Y. Weng, and D. N. Sheng, Phys. Rev. Lett.**101**, 117203 (2008).
[8] S. Nishimoto, N. Shibata, and C. Hotta, Nature Comm. **4**, 2287 (2013).
[9] S. Capponi, O. Derzhko, A. Honecker, A. M. Läuchli, and J. Richter, Phys. Rev. B **88**, 144416(R) (2013).
[10] I. Affleck, T. Kennedy, E. H. Lieb, and H. Tasaki, Phys. Rev. Lett. **59**, 799 (1987); Commun. Math. Phys. **115**, 477 (1988).
[11] H. Asakawa and M. Suzuki, Physica A **198**, 210 (1993).
[12] K. Hida, J. Phys. Soc. Jpn. **69**, 4003 (2000); **70**, 3673 (2001).
[13] W. Li, S. Yang, M. Cheng, Z.-X.Liu, and H.-H. Tu, Phys. Rev. B**89**, 174411 (2014)
[14] N. Wada, T. Kobayashi, H. Yano, T. Okuno, A. Yamaguchi, and K. Awaga, J. Phys. Soc. Jpn. **66**, 961 (1997).
[15] T. Matsushita, N. Hamaguchi, K. Shimizu, N. Wada, W. Fujita, K. Awaga, A. Yamaguchi, and H. Ishimoto, J. Phys. Soc. Jpn. **79**, 093701 (1997).
[16] S. Hara, H. Sato, and Y. Narumi, J. Phys. Soc. Jpn.**81**, 073707 (2012).
[17] J. N. Behera and C. N. R. Rao, J. Am. Chem. Soc. **128**, 9334 (2006).
[18] D. Papoutsakis, D. Grohol, and D.G. Nocera, J. Am. Chem. Soc. **124**, 2647 (2002).
[19] S. Gong, W. Zhu, and D. N. Sheng, arXiv:1312.4519v1.
[20] R. Ganesh, J. van den Brink, and S. Nishimoto, Phys. Rev. Lett. **110**, 127203 (2013).
[21] M. Oshikawa and T. Senthil, Phys. Rev. Lett.**96**, 060601 (2006).
[22] A. Kitaev, and J. Preskill, Phys. Rev. Lett.**96**, 110404 (2006).
[23] M. Levin and X. G. Wen, Phys. Rev. Lett.**96**, 110405 (2006).
[24] Z. Cai, S. Chen, and Y. Wang, J. Phys.: Condens. Matter **21**, 456009 (2009).
[25] H. J. Changlani and A. M. Läuchli, arXiv:1406.4767v1.
[26] T. Liu, W. Li, A. Weichselbaum, J. von Delft, and G. Su, arXiv:1406.5905v1.

CYLINDRICAL CLUSTERS

In this Letter, we follow the notation of cylindrical cluster in Ref. 2. A cylinder is labeled as XCn (YCn) when the circumference is along or close in orientation to the $x(y)$-axis, where n is the circumference in unit of the lattice spacing. If the lattice is connected with a shift d units in the periodic direction, the number of shift is added to the label such as XCn-d.

In Fig. 6 several kinds of the cylindrical cluster are illustrated. Some arbitrariness remains on the shape of open edges. For example, the lattices (a) and (b) are both labeled by the XC8 cylinders but the shapes of the open edges are different. One of them has hexagons and the other has triangles at the open edges. Then, there is a possibility that the hexagonal singlet or triangular Haldane-gap dimers is artificially favoured. If we choose the XCn-(n/2) type of cylinder, the hexagons and triangulars may be *equally* placed at the open edges, as shown in Fig. 6(c). Also, a kind of the YCn cylinder [Fig. 6(d)] has the similar edges. Another kind of the YCn cylinder like in Fig. 6(e) has triangles at the open edges, and however, it could be useful cluster to detect the TVBS state directly as a translation-symmetry-breaking state along the OBC direction.

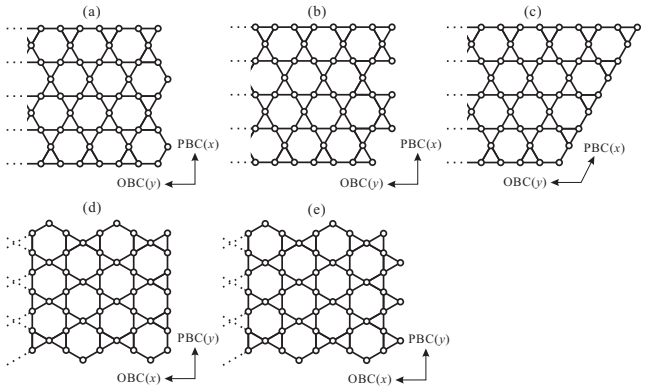

FIG. 6. (a),(b) Kinds of XC8 cylinders. (c) A kind of XC8-4 cylinder. (d),(e) Kinds of YC6 cylinders.

PERIODIC CLUSTERS

In Fig. 7 the periodic clusters used in our numerical calculations are shown. They are taken as isotropic as possible. As shown in the main text, the $N = 36$ periodic cluster is completely isotropic.

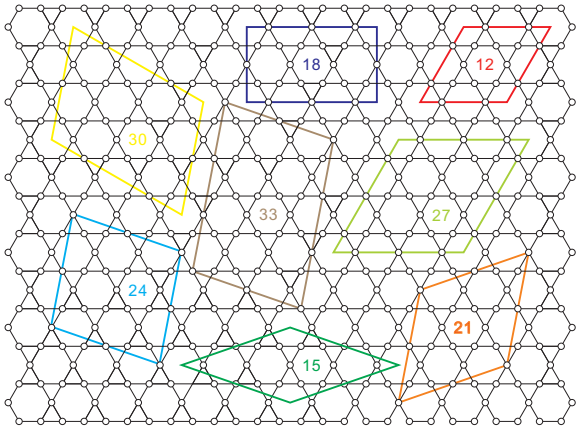

FIG. 7. Periodic clusters used in our numerical calculations.